

Bath engineering enhanced quantum critical engines

Revathy B. S,¹ Victor Mukherjee,² and Uma Divakaran¹

¹*Department of Physics, Indian Institute of Technology Palakkad, Palakkad, 678557, India*

²*Department of Physical Sciences, IISER Berhampur, Berhampur 760010, India*

(Dated: August 16, 2022)

Driving a quantum system across quantum critical points leads to non-adiabatic excitations in the system. This in turn may adversely affect the functioning of a quantum machine which uses a quantum critical substance as its working medium. Here we propose *Bath Engineered Quantum Engine* (BEQE), where we use Kibble-Zurek mechanism to formulate a protocol for enhancing the performance of finite-time quantum engines operating close to quantum phase transitions. In case of free-Fermionic systems, BEQE enables finite-time engines to outperform engines operating in presence of shortcut to adiabaticity, and even infinite-time engines under suitable conditions, thus showing the remarkable advantage offered by this technique. Open questions remain in case of BEQE based on non-integrable models.

I. INTRODUCTION

The field of quantum thermodynamics aims to form a coherent understanding of the thermodynamics of quantum systems [1–7]. As for the case of classical thermodynamics, one can then use this knowledge to understand the limitations on the performance of quantum machines. In this respect, quantum control can play a significant role in enabling us to go beyond these limitations, and develop high performing quantum machines [8, 9]. This can be specially significant in case of finite-time quantum machines [10, 11], where non-adiabatic excitations may be detrimental to the performances of such machines, thus necessitating the application of control in order to boost their outputs [12, 13].

Control techniques such as shortcuts to adiabaticity (STA), have been shown to be highly successful in enhancing the output of finite-time quantum engines [14–19]. However, application of STA can be highly non-trivial in many-body quantum engines, owing to the diverging dimensions of the associated Hilbert spaces. This can be specially challenging in quantum engines operating close to quantum critical points, where the diverging length and time scales can demand STA protocols involving long-range interactions [20, 21]. The above challenges motivate us to search for control protocols beyond STA, for application in quantum engines operating close to quantum phase transitions.

In this work we propose a control protocol aimed at enhancing the efficiency as well as output work of quantum engines based on free-Fermionic WMs, operating close to quantum critical points [22]. Quantum phase transitions has proven to be beneficial for quantum heat engines [23–26]. The universality in quantum critical machines arising from Kibble Zurek mechanism (KZM) has already been studied in [27]. We construct a quantum heat engine using working medium that undergoes quantum phase transition. The formation of excitations close to the critical point due to the divergence of relaxation time results in loss of adiabaticity, thus reducing the performance of the quantum machine [28–30]. While

conventional control techniques like STA involve complex calculations and non-trivial many-body interactions, we propose implementation of *Bath Engineered Quantum Engine* (BEQE), in which the working of the engine can be improved significantly through simple control of bath spectral functions.

The present work is organized as follows: we describe a many body quantum Otto cycle in Sec. II. In Sec. III, operation of BEQE using a generic free-Fermionic WM is explained in detail ; we study a specific example of BEQE using transverse Ising model in Sec. IV. Finally we summarize our results in Sec. V. Details of the calculations presented in this work are included in the Appendix.

II. MANY BODY QUANTUM OTTO CYCLE

We consider an Otto cycle with the working medium (WM) described by the Hamiltonian $H(\lambda(t))$, where λ is a time dependent parameter. The four stroke quantum Otto cycle consists of two non-unitary strokes and two unitary strokes, as described below (Fig. 1):

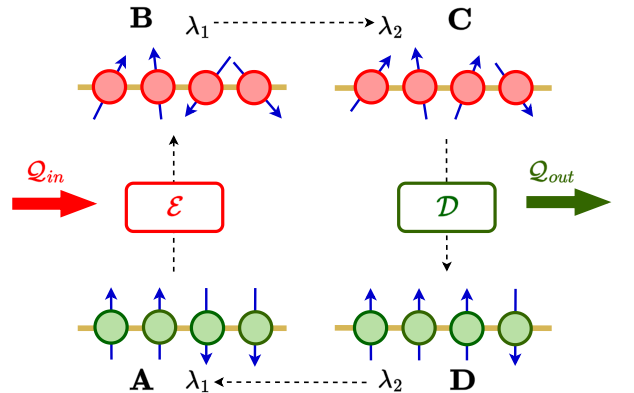


FIG. 1. Schematic diagram of a quantum Otto cycle with a many-body spin system as the working medium.

(i) Non-unitary stroke A \rightarrow B: The WM with pa-

parameter $\lambda = \lambda_1$ is connected to an energizing bath \mathcal{E} till it reaches the corresponding steady state at \mathbf{B} by receiving energy \mathcal{Q}_{in} from the bath.

- (ii) *Unitary stroke $\mathbf{B} \rightarrow \mathbf{C}$* : The WM is decoupled from the energizing bath and λ is changed from λ_1 to λ_2 at a speed $1/\tau_1$.

This unitary evolution is described by the von-Neumann equation of motion:

$$\frac{d\rho}{dt} = -i[H, \rho]. \quad (1)$$

- (iii) *Non-unitary stroke $\mathbf{C} \rightarrow \mathbf{D}$* : The WM with $\lambda = \lambda_2$ is now connected to a decaying bath \mathcal{D} till it reaches the corresponding steady state at \mathbf{D} ; energy \mathcal{Q}_{out} flows from the WM to the bath during this stroke.

- (iv) *Unitary stroke $\mathbf{D} \rightarrow \mathbf{A}$* : After decoupling from the decaying bath, the parameter λ is changed back to λ_1 from λ_2 with a speed $1/\tau_2$.

The energy at the end of stroke i is calculated using the equation

$$E_i = \text{Tr}(H^i \rho^i) \quad (2)$$

where H^i and ρ^i are the Hamiltonian and the density matrix at $i = \mathbf{A}, \mathbf{B}, \mathbf{C}, \mathbf{D}$. The heat input (\mathcal{Q}_{in}) and heat output (\mathcal{Q}_{out}) can be calculated using

$$\mathcal{Q}_{in} = E_B - E_A \quad (3)$$

$$\mathcal{Q}_{out} = E_D - E_C. \quad (4)$$

The output work is given by $\mathcal{W} = -(\mathcal{Q}_{in} + \mathcal{Q}_{out})$. The sign convention used here is, energy is taken to be positive (negative) if it enters (leaves) the WM. The Otto cycle works as an engine when $\mathcal{Q}_{in} > 0$, $\mathcal{Q}_{out} < 0$ and $|\mathcal{W}| < 0$. The performance of the engine is then characterised using the quantity, efficiency (η) which is defined as

$$\eta = -\frac{\mathcal{W}}{\mathcal{Q}_{in}}. \quad (5)$$

III. BATH SPECTRAL FORM ENGINEERING

We consider a free-Fermionic WM, described by a Hamiltonian of the form

$$H = \sum_k \psi_k^\dagger H_k \psi_k$$

$$H_k = \vec{f}(k) \cdot \vec{\sigma}_k \quad (6)$$

where $\vec{\sigma}_k = (\sigma_k^x, \sigma_k^y, \sigma_k^z)$ denotes the Pauli matrices corresponding to the k -th mode, $\vec{f}(k)$ is a model-dependent function for the k -th mode, and $\psi_k^\dagger = (c_{1k}^\dagger \ c_{2k}^\dagger)$, where c_{jk} and c_{jk}^\dagger (with $j = 1, 2$) denote the fermionic operators corresponding to the k -th mode.

For non-interacting k modes, the density matrix ρ of the system can be written as $\rho = \otimes_k \rho_k$. The WM undergoes unitary dynamics during the strokes $\mathbf{D} \rightarrow \mathbf{A}$ and $\mathbf{B} \rightarrow \mathbf{C}$, described by the von-Neumann equation

$$\dot{\rho}_k = -i[H_k, \rho_k] \quad (7)$$

for each k mode. Further, we assume Fermionic baths such that each k mode evolves independently during the non-unitary strokes, described by the master equation [31]

$$\frac{d\rho_k}{dt} = \mathcal{G}_\alpha(\Delta_k) \mathcal{L}_k[\rho_k(t)] + \mathcal{G}_\alpha(-\Delta_k) \mathcal{L}_k^\dagger[\rho_k(t)] \quad (8)$$

where following the Kubo-Martin-Schwinger condition, $\mathcal{G}_\alpha(-\Delta_k) = \exp(\Delta_k/T_\alpha) \mathcal{G}_\alpha(\Delta_k)$. Here $\mathcal{G}_\alpha(\nu)$ denotes the spectral function of the $\alpha = \mathcal{E}, \mathcal{D}$ bath at frequency ν , while T_α is the effective temperature of the α bath [27, 32]. The superoperator \mathcal{L}_k is of the form

$$\mathcal{L}_k = \left(L_k \rho_k L_k^\dagger - \frac{1}{2} \{L_k^\dagger L_k, \rho_k\} \right) \quad (9)$$

with L_k being the Lindblad operators denoting jumps between the different eigenenergy levels. The above dynamics given in Eq. (8) ensures that each k mode thermalizes independently with the bath, such that the steady state of the WM at the end of an isochoric stroke is given by $\rho = \otimes_k \rho_k^{\text{th}}$, where ρ_k^{th} is the Gibbs state corresponding to the k -th mode [33].

Non-adiabatic excitations are inevitable when a quantum system is driven across quantum critical points [28]. This results in reduction of output work as well as efficiency when a quantum critical substance is made the working medium of a quantum Otto engine [27]. Here, we propose bath spectral form engineering to prevent these excitations from reducing the performance of the engine, henceforth called *Bath Engineered Quantum Engine* (BEQE).

In the bath engineering technique we choose bath spectral functions \mathcal{G}_α with appropriate cut-offs, such that the modes which have higher probabilities of getting excited, and therefore are detrimental to the performance of the finite-time quantum engine, are not allowed to participate in the dynamics. While techniques like shortcuts to adiabaticity are applied in the unitary strokes, bath engineering is performed during the non-unitary strokes (Fig. 2 (a)).

The physics of excitations generated in a system which is driven at a finite rate across a quantum critical point (QCP) is well established and is described by the Kibble Zurek mechanism (KZM) [30, 34, 35]. According to the adiabatic-impulse approximation [36], these excitations occur due to vanishing energy gaps which are below a threshold value (say, Δ^*), the expression of which can be obtained using KZ arguments as described below. Bath engineering is done such that the energy levels having gaps less than Δ^* are not allowed to interact with the bath, i.e, $\mathcal{G}(\Delta_k < \Delta^*) \approx 0$, thus preventing them from participating in the operation of the cycle (Fig. 2 (b)).

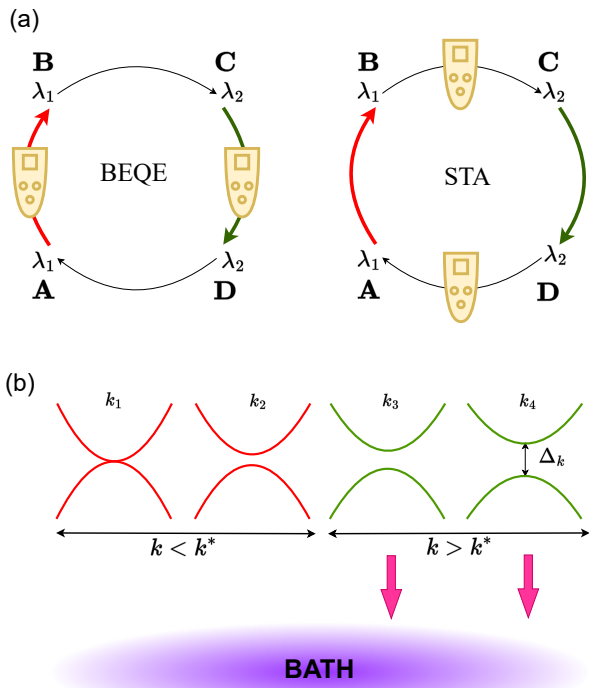


FIG. 2. (a) Schematic diagram showing bath engineering being applied during the non-unitary strokes, whereas shortcuts to adiabaticity is applied during the unitary strokes. (b) A k mode gets coupled to the bath if $\Delta_k > \Delta^*$ ($k > k^*$) and not coupled to the bath if $\Delta_k < \Delta^*$ ($k < k^*$) where $\Delta_{k^*} = \Delta^*$.

Kibble Zurek mechanism assisted BEQE

According to KZM, the response of a system driven across a quantum critical point is determined by the inherent time scale (relaxation time ξ_τ) of the system, and the rate of change of the system Hamiltonian [36]; when the relaxation time ξ_τ of the system is greater than the rate at which the Hamiltonian parameter λ is changed, the system stops evolving adiabatically, thus resulting in non-adiabatic excitations. In order to arrive at a more quantitative analysis, let us assume t^* is the time at which the system loses adiabaticity and excitations begin to occur. The energy gap Δ_{k_c} at the critical mode k_c scales with the distance from the critical point λ_c as

$$\Delta_{k_c} \sim (\lambda - \lambda_c)^{\nu z}, \quad (10)$$

where ν and z are the correlation length and dynamical critical exponents, respectively. When the parameter λ is varied using the quench protocol $\lambda = \lambda_2 + (\lambda_1 - \lambda_2)\frac{t}{\tau}$, one can write

$$\lambda - \lambda_c = \lambda_2 - \lambda_c + (\lambda_1 - \lambda_2)\frac{t}{\tau}. \quad (11)$$

The time t^* is determined by the condition that the relaxation time ξ_τ is of the order of the time scale with

which λ is changed, i.e.,

$$\frac{\Delta_{k_c}}{\dot{\Delta}_{k_c}} \Big|_{t=t^*} \sim \xi_\tau. \quad (12)$$

Further, the relaxation time diverges according to the scaling

$$\xi_\tau \sim \frac{1}{\Delta_{k_c}} \sim (\lambda - \lambda_c)^{-\nu z}. \quad (13)$$

Using the expressions (10) - (13) one gets,

$$\begin{aligned} \frac{\Delta_{k_c}}{\dot{\Delta}_{k_c}} \Big|_{t=t^*} &\sim \frac{(\lambda_2 - \lambda_c) + (\lambda_1 - \lambda_2)\frac{t^*}{\tau}}{\nu z \left(\frac{\lambda_1 - \lambda_2}{\tau}\right)} \\ \Rightarrow t^* &\sim \frac{\tau}{\lambda_1 - \lambda_2} \left[(\lambda_c - \lambda_2) \right. \\ &\quad \left. + \left(\nu z \left(\frac{\lambda_1 - \lambda_2}{\tau}\right) \right)^{\frac{1}{1+\nu z}} \right] \end{aligned} \quad (14)$$

Thus, the energy gap at which the excitations begin to happen for the critical mode is given by

$$\Delta^* = \Delta_{k_c} \Big|_{t^*} \sim \left(\frac{\nu z (\lambda_1 - \lambda_2)}{\tau} \right)^{\frac{\nu z}{1+\nu z}}. \quad (15)$$

In the quantum Otto cycle, bath engineering is implemented during the non-unitary strokes $\mathbf{C} \rightarrow \mathbf{D}$ and $\mathbf{A} \rightarrow \mathbf{B}$ by choosing

$$\begin{aligned} \mathcal{G}_{\mathcal{D}}(\Delta_k) &\approx 0 && \text{for } \Delta_k < \Delta^* \\ \mathcal{G}_{\mathcal{E}}(\Delta_k) &\approx 0 && \text{for } \Delta_k < \gamma \Delta^* \end{aligned} \quad (16)$$

respectively, such that small energy gaps which have higher probability of getting excited do not participate in the dynamics. Here γ is the scaling factor by which a typical energy gap changes in the $\mathbf{D} \rightarrow \mathbf{A}$ stroke.

Now we demonstrate bath engineering technique using a free Fermionic model which is described in the following section.

IV. BEQE WITH TRANSVERSE ISING MODEL AS WM

A prototypical example for a free-Fermionic system undergoing quantum phase transition is the one dimensional transverse Ising model (TIM). It is an exactly solvable model and thus widely studied. The Hamiltonian of the transverse Ising model is

$$H(t) = -J \sum_n \sigma_n^x \sigma_{n+1}^x - h(t) \sum_n \sigma_n^z \quad (17)$$

with J being the nearest neighbour interaction strength, $h(t)$ is the transverse field that is time dependent playing the role of λ in the previous section, and n is the lattice site index. Here, σ_n^i with $i = x, y, z$ are the Pauli matrices at each site n . This system shows zero temperature

quantum phase transition from paramagnetic to ferromagnetic state at the quantum critical point $h = \pm J$ [37–39].

After doing Jordan - Wigner fermionization and taking the Fourier transform, the Hamiltonian H_k takes the form [38]:

$$H_k = -2(h - \cos k) \sigma^z + 2 \sin k \sigma^x. \quad (18)$$

Even though unitary dynamics allows transitions only between $|0\rangle$ and $|k, -k\rangle = c_k^\dagger c_{-k}^\dagger |0\rangle$, the system bath interactions lead to transitions to the $|\pm k\rangle = c_{\pm k}^\dagger |0\rangle$ states as well, resulting in mixing of states [31, 40]. Therefore, the Hamiltonian is rewritten in the basis $|0\rangle, |k\rangle, |-k\rangle, |k, -k\rangle$ as

$$H_k = \begin{bmatrix} -2(h - \cos k) & 0 & 0 & 2 \sin k \\ 0 & 0 & 0 & 0 \\ 0 & 0 & 0 & 0 \\ 2 \sin k & 0 & 0 & 2(h - \cos k) \end{bmatrix} \quad (19)$$

with eigenenergies $-\epsilon_k, 0, 0, \epsilon_k$ where $\epsilon_k = 2\sqrt{(h - \cos k)^2 + \sin^2 k}$.

We now focus on the strokes of the Otto cycle with the TIM as the WM. The density matrix at **B** is given by $\rho^B (= \otimes_k \rho_k^B)$, where

$$\rho_k^B = \begin{bmatrix} \frac{e^{\beta\epsilon_k}}{Z_k} & 0 & 0 & 0 \\ 0 & \frac{1}{Z_k} & 0 & 0 \\ 0 & 0 & \frac{1}{Z_k} & 0 \\ 0 & 0 & 0 & \frac{e^{-\beta\epsilon_k}}{Z_k} \end{bmatrix} \quad (20)$$

is the thermal state for the mode k corresponding to $T = T_H$ and $h = h_1$. Here $\beta = \frac{1}{k_B T_H}$, (k_B is set to unity for the rest of the paper) and $Z_k = 2 + e^{\beta\epsilon_k} + e^{-\beta\epsilon_k}$ is the partition function for each k mode. In the unitary stroke (**B** \rightarrow **C**), the transverse field is changed from h_1 to h_2 according to the protocol,

$$h(t) = h_1 + (h_2 - h_1) \left(\frac{t}{\tau_1} \right), \quad t \in [0, \tau_1] \quad (21)$$

in a time τ_1 with $h_1 \gg h_2$. During the non-unitary stroke (**C** \rightarrow **D**) the system again reaches a state $\rho^D = \otimes_k \rho_k^D$, where ρ_k^D is the thermal state for the mode k corresponding to T_C and $h = h_2$ at **D**. The transverse field h_2 is then changed back to h_1 using the same quench protocol but in time τ_2 in the unitary stroke **D** \rightarrow **A**.

Now let us examine how bath engineering is implemented in TIM. As discussed before, we make use of selective coupling between the bath and working medium so that some k modes close to the critical mode k_c having energy gap Δ_k lower than the threshold value Δ^* ($= \left(\frac{\nu z (h_1 - h_2)}{\tau} \right)^{\frac{\nu z}{1 + \nu z}}$), is prohibited from interacting with the bath thereby preventing these modes from

thermalizing.

The energy gap between $|0\rangle$ and $|k, -k\rangle$ states for each k mode is given by

$$\Delta_k = 2\epsilon_k = 4\sqrt{(h - \cos k)^2 + \sin^2 k}. \quad (22)$$

For TIM, the critical exponents are $\nu = 1$ and $z = 1$ so that Δ^* as obtained in Eqn. 15 is given by

$$\Delta^* = \sqrt{\frac{h_1 - h_2}{\tau_2}} \quad (23)$$

Below we present the steps to incorporate bath engineering in the quantum Otto cycle,

a) As discussed above, we consider a lower cut-off for the decaying bath spectral function, given by $\mathcal{G}_D(\Delta) \approx 0$ for $\Delta_k < \Delta^*$ (see Eqs. (16) and (23)). This choice of bath spectral function ensures that modes with $\Delta_k < \Delta^*$ are not allowed to interact with the decaying bath, so that $\rho_k^D = \rho_k^C$ for these modes.

On the other hand, modes with $\Delta_k > \Delta^*$ thermalize with the decaying bath and reach the state $\rho_k^D = \frac{e^{-\beta_C H_k(h_2)}}{Z_k}$ at **D**.

b) In the **D** \rightarrow **A** stroke, the Hamiltonian is changed from h_2 to h_1 , starting from the state ρ_k^D to reach ρ_k^A .

c) At **A**, the lower cutoff for the energizing bath is chosen to be $\mathcal{G}_E \approx 0$ for $\Delta_k < \gamma \Delta^*$ where γ is chosen in such a way that $\gamma \Delta^*$ is of the order of the lower energy gaps for $h = h_1$ which allows for some modes to be bath engineered in the energizing bath stroke. This results in $\rho_k^B = \rho_k^A$ for such modes.

The modes with $\Delta_k > \gamma \Delta^*$ are allowed to interact with the energizing bath leading the system to the steady state given by Eqn. 20.

d) from **B** to **C**, the system is quenched and all modes evolve to reach ρ^C .

The total heat input and output of the system is calculated using

$$\mathcal{Q}_{in} = \sum_k \mathcal{Q}_{in}^k \quad (24)$$

$$\mathcal{Q}_{out} = \sum_k \mathcal{Q}_{out}^k \quad (25)$$

and the work output and efficiency of the engine is obtained using

$$\mathcal{W} = - \left(\sum_k \mathcal{Q}_{in}^k + \sum_k \mathcal{Q}_{out}^k \right) \quad (26)$$

$$\eta = - \frac{\mathcal{W}}{\sum_k \mathcal{Q}_{in}^k} \quad (27)$$

We study the variation of output work and efficiency of the engine after implementing bath engineering in Fig. 3. To have a complete picture, we compare BEQE with finite time engines without any control, finite time engines in presence of shortcuts to adiabaticity in the unitary strokes and engines operating in the adiabatic limit, i.e. $\tau_1 = \tau_2 = \tau \rightarrow \infty$ (or infinite time engines). As shown in [41], the STA Hamiltonian involves long-range interactions. However, one can truncate the control Hamiltonian to M body terms, to have a physically realizable approximate STA protocol. In Fig. 3, we present a comparison of the output work as a function of τ ($= \tau_1 = \tau_2$). As expected, STA used engines always perform better than the finite-time engines without control. However, interestingly, the BEQE outperforms STA used engines, as well as the perfectly adiabatic engine, for a wide range of τ values, thus exhibiting the remarkable benefit offered by the bath engineering technique.

Similarly, we also plot efficiency η as a function of τ (see inset of Fig. 3) and compare BEQE with engines operating with different techniques. As in the case of work output, here also we find that BEQE outperforms all other engines for the same range of τ values as in work output. The expressions for $|\mathcal{W}|_{adia}$ and η_{adia} are given in appendix A.

BEQE outperforming other engines can be explained using Fig. 4 where \mathcal{Q}_{in} and \mathcal{Q}_{out} for a perfect adiabatic engine is plotted as a function of individual k modes. In Fig. 4, it can be seen that even when the engine works in the adiabatic limit, there are some k modes close to the critical mode which do not function as an 'engine' ($\mathcal{Q}_{in} < 0$). To understand this better, let us consider the adiabatic limit where $\rho_k^C = \rho_k^B$ in the eigenbasis. In this limit, \mathcal{Q}_{in} for each k mode is given by (see appendix A for details)

$$\mathcal{Q}_{in}^k = \frac{\Delta_k(h_1)}{2} \left[\frac{e^{-\frac{\beta_H \Delta_k(h_1)}{2}} - e^{\frac{\beta_H \Delta_k(h_1)}{2}}}{Z(h_1)} - \frac{e^{-\frac{\beta_C \Delta_k(h_2)}{2}} - e^{\frac{\beta_C \Delta_k(h_2)}{2}}}{Z(h_2)} \right] \quad (28)$$

For \mathcal{Q}_{in}^k to be positive,

$$\frac{\sinh(\frac{\beta_H \Delta_k(h_1)}{2})}{2 + \cosh(\frac{\beta_H \Delta_k(h_1)}{2})} < \frac{\sinh(\frac{\beta_C \Delta_k(h_2)}{2})}{2 + \cosh(\frac{\beta_C \Delta_k(h_2)}{2})}. \quad (29)$$

There can be modes for which this condition is not satisfied, resulting in 'non engine' modes in the adiabatic limit. BEQE helps to remove these non-engine modes from participating in the non-unitary strokes, thereby boosting the performance of the engine compared to the perfectly adiabatic engine. It is to be noted that the presence of non-engine modes are essential for BEQE to outperform adiabatic engine. For instance, when $T_H \rightarrow \infty$ ($\beta_H \rightarrow 0$), Eq. 29 may be satisfied for all modes so that the technique of BEQE will not give better results compared to adiabatic engine. However we emphasize

that while Eq. (29) and the discussion above are specific to TIM WM, BEQE can be expected to perform better than generic finite time free-Fermionic quantum critical engines, following the arguments presented in Sec. III.

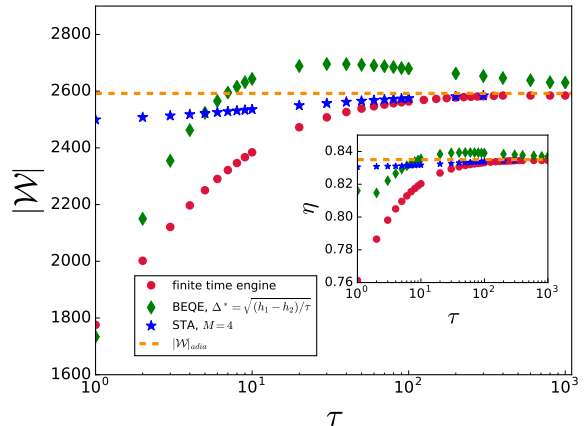


FIG. 3. $|\mathcal{W}|$ is plotted as a function of τ for the critical engine using different techniques. Inset: η is plotted as a function of τ . The parameters used are $L = 1000, h_1 = 10, h_2 = 1, T_H = 20, T_C = 1, \gamma = 6.5, \tau_1 = \tau_2 = \tau$.

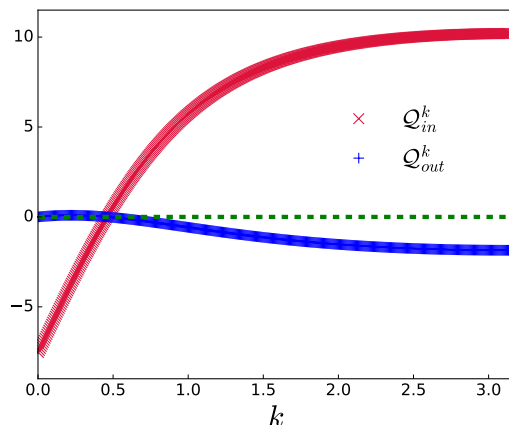


FIG. 4. \mathcal{Q}_{in}^k and \mathcal{Q}_{out}^k are plotted as functions of k modes for the critical engine in the adiabatic limit. The parameters are $L = 1000, h_1 = 10, h_2 = 1, T_H = 20, T_C = 1$. The green dashed line represents the zero of heat.

We note that BEQE depends on appropriate choice of bath spectral function (16), which again depends on τ through Eq. (15). However, in experimental setups, it might be difficult to change the bath-spectral function for every change of τ . Consequently, we examine the robustness of the bath engineering protocol by plotting the work output and efficiency vs τ for constant values of Δ^* . In this case also, the results show that the engine performance can be enhanced by choosing appropriate constant values of Δ^* as shown in Fig. 5, thus highlighting the effectiveness of the proposed protocol in practical scenarios.

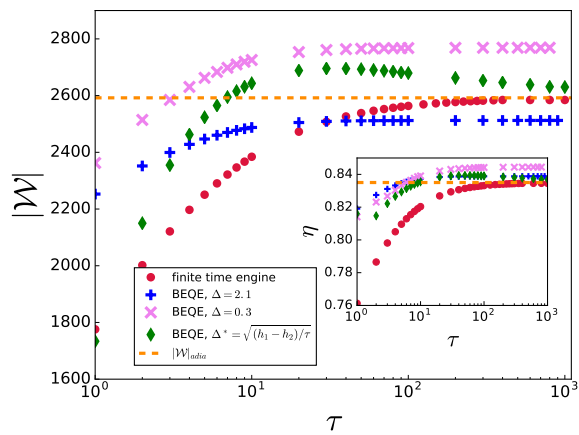


FIG. 5. $|\mathcal{W}|$ is plotted as a function of τ using constant value of Δ^* for all τ . Inset: η is plotted as a function of τ . Here, $\gamma(\Delta^* = 2.1) = 9$ and $\gamma(\Delta^* = 0.3) = 62$. Other parameters are same as in Fig. 3.

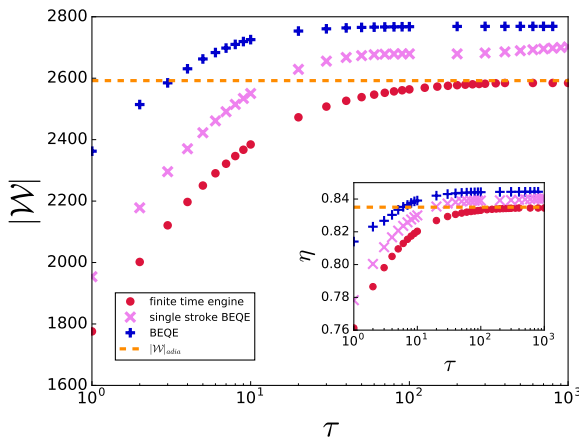


FIG. 6. $|\mathcal{W}|$ is plotted as a function of τ using constant value of Δ^* for all τ with bath engineering only in the $\mathbf{C} \rightarrow \mathbf{D}$ non-unitary stroke (single stroke BEQE) and with bath engineering in both the non-unitary strokes (BEQE). Inset: η is plotted as a function of τ . Here $\Delta^* = 0.3, \gamma = 62$. Other parameters are same as in Fig. 3.

We point out that one may be able to further simplify the control protocol by implementing bath engineering in only one of the non-unitary strokes (single stroke BEQE). From Fig. 6, it is seen that even single stroke BEQE is also performing better than the finite and infinite time engines. Therefore, this simplified protocol can be helpful as long as the overall work output can be increased, which one can calculate following the mechanism discussed above, even though there might be scenarios in which this simplified protocol may not suffice.

V. CONCLUSION

We have proposed Bath Engineered Quantum Engine, where through appropriate choice of bath spectral functions, one can dramatically boost the performance of quantum critical engines based on free-Fermionic WMs. The operation of BEQE inherently depends on the Kibble-Zurek mechanism; consequently, knowledge about the universality class of the WM and the strokes of the Otto cycle suffice to implement this method. This can be in stark contrast to conventional methods such as shortcuts to adiabaticity, where one might need detailed knowledge about the eigenspectrum for its application. We emphasize that the improvement in performance in case of BEQE is also accompanied by significant reduction in complexity in formulating the control protocol, as compared to more conventional techniques, such as STA, which can involve non-trivial many-body terms in quantum systems driven through quantum critical points [19–21]. Furthermore, interestingly, in spite of the simplicity of the proposed control protocol, our analysis with TIM WM shows that BEQE can outperform quantum engines assisted through STA, and even infinite-time quantum engines, thus highlighting the significant benefits offered by this control method. We also exhibit the robustness of the BEQE control protocol by considering constant values of τ .

Several existing setups can be suitable for experimental realization of BEQE, such as trapped ions [42–46], optical lattices [47], superconducting qubits, nitrogen vacancy centers in diamond [48], NMR qubit systems [49], etc. For example, quantum simulators based on trapped ions have already been used to study Kibble-Zurek mechanism in the momentum space [50].

Finally, we note that while this technique appears to be highly successful in case of free-Fermionic WMs, open questions remain in case of its application with non-integrable WMs, where such non-interacting k modes may not exist. For example, one can choose the WM to be the antiferromagnetic transverse Ising model with longitudinal field (LTIM), described by the Hamiltonian

$$H = J \sum_i \sigma_i^z \sigma_{i+1}^z - B_x(t) \sum_i \sigma_i^x - B_z \sum_i \sigma_i^z. \quad (30)$$

Here J is the strength of antiferromagnetic interaction, B_z is a longitudinal field and B_x denotes a time dependent transverse field. The competition between J and B_z leads to a quantum phase transition from the antiferromagnetic state to the paramagnetic state at a critical value of B_x^c for a fixed value of B_z [51, 52]. One can model an Otto cycle using LTIM WM and implement BEQE as described above (see App. B). However, preliminary studies suggest that, unlike the case of integrable model, there is no improvement in the output of the BEQE in this case (see Fig. 7). This can be attributed to the absence of non-interacting momentum modes, as obtained for free-Fermionic systems. However, additional rigorous studies are needed to have a deeper understanding of

the possibility of the application of BEQE to quantum engines based on more generic non-integrable WMs.

ACKNOWLEDGMENTS

V.M. acknowledges support from Science and Engineering Research Board (SERB) through MATRICS (Project No. MTR/2021/000055) and Seed Grant from IISER Berhampur.

Appendix A: Adiabatic evolution of TIM

The energies at the end of stroke i are calculated using the expression

$$E_i = \sum_k \text{Tr}[H_k^i \rho_k^i]. \quad (\text{A1})$$

where $i = \mathbf{A}, \mathbf{B}, \mathbf{C}, \mathbf{D}$.

- (i) **At B:** The density matrix is given by Eqn (20) and the Hamiltonian in the diagonal basis takes the form

$$H_k(h_1) = \begin{bmatrix} -\epsilon_k(h_1) & 0 & 0 & 0 \\ 0 & 0 & 0 & 0 \\ 0 & 0 & 0 & 0 \\ 0 & 0 & 0 & \epsilon_k(h_1) \end{bmatrix}. \quad (\text{A2})$$

The energy E_B can be calculated as follows

$$\text{Tr}[H_k(h_1) \rho_k^B] = \frac{\epsilon_k(h_1)}{Z(h_1)} \left(e^{-\beta_H \epsilon_k(h_1)} - e^{\beta_H \epsilon_k(h_1)} \right) \quad (\text{A3})$$

or

$$E_B = \sum_k \text{Tr}[H_k(h_1) \rho_k^B] \quad (\text{A4})$$

$$= \sum_k \frac{\epsilon_k(h_1)}{Z(h_1)} \left(e^{-\beta_H \epsilon_k(h_1)} - e^{\beta_H \epsilon_k(h_1)} \right) \quad (\text{A5})$$

- (ii) **At C:** If the evolution is purely adiabatic, the populations in the eigenenergy levels do not change resulting to

$$\rho_k^{C,adia} = \rho_k^B = \begin{bmatrix} \frac{e^{\beta_H \epsilon_k(h_1)}}{Z(h_1)} & 0 & 0 & 0 \\ 0 & \frac{1}{Z(h_1)} & 0 & 0 \\ 0 & 0 & \frac{1}{Z(h_1)} & 0 \\ 0 & 0 & 0 & \frac{e^{-\beta_H \epsilon_k(h_1)}}{Z(h_1)} \end{bmatrix} \quad (\text{A6})$$

and

$$H_k(h_2) = \begin{bmatrix} -\epsilon_k(h_2) & 0 & 0 & 0 \\ 0 & 0 & 0 & 0 \\ 0 & 0 & 0 & 0 \\ 0 & 0 & 0 & \epsilon_k(h_2) \end{bmatrix} \quad (\text{A7})$$

with $\epsilon_k(h_2) = 2\sqrt{(h_2 - \cos k)^2 + \sin k^2}$.
Therefore,

$$E_C^{adia} = \sum_k \frac{\epsilon_k(h_2)}{Z(h_1)} \left(e^{-\beta_H \epsilon_k(h_1)} - e^{\beta_H \epsilon_k(h_1)} \right) \quad (\text{A8})$$

- (iii) **At D:** This energy can be calculated similar to that at **B** so that

$$E_D = \sum_k \frac{\epsilon_k(h_2)}{Z(h_2)} \left(e^{-\beta_C \epsilon_k(h_2)} - e^{\beta_C \epsilon_k(h_2)} \right) \quad (\text{A9})$$

- (iv) **At A:** Following the same procedure used to calculate the energy E_C^{adia} in order to find the energy E_A^{adia} , we get

$$E_A^{adia} = \sum_k \frac{\epsilon_k(h_1)}{Z(h_2)} \left(e^{-\beta_C \epsilon_k(h_2)} - e^{\beta_C \epsilon_k(h_2)} \right) \quad (\text{A10})$$

The input heat energy absorbed by the WM in the non-unitary stroke $\mathbf{A} \rightarrow \mathbf{B}$ can be easily calculated, and is given by

$$\begin{aligned} \mathcal{Q}_{in}^{adia} &= E_B - E_A^{adia} \\ &= \sum_k \epsilon_k(h_1) \left\{ \frac{(e^{-\beta_H \epsilon_k(h_1)} - e^{\beta_H \epsilon_k(h_1)})}{Z(h_1)} \right. \\ &\quad \left. - \frac{(e^{-\beta_C \epsilon_k(h_2)} - e^{\beta_C \epsilon_k(h_2)})}{Z(h_2)} \right\} \end{aligned} \quad (\text{A11})$$

Similarly,

$$\begin{aligned} \mathcal{Q}_{out}^{adia} &= E_D - E_C^{adia} \\ &= \sum_k \epsilon_k(h_2) \left\{ \frac{(e^{-\beta_C \epsilon_k(h_2)} - e^{\beta_C \epsilon_k(h_2)})}{Z(h_2)} \right. \\ &\quad \left. - \frac{(e^{-\beta_H \epsilon_k(h_1)} - e^{\beta_H \epsilon_k(h_1)})}{Z(h_1)} \right\}. \end{aligned} \quad (\text{A12})$$

We can now calculate the output work of the engine in the adiabatic limit which is given by

$$\begin{aligned} |\mathcal{W}|_{adia} &= \sum_k (\epsilon_k(h_1) - \epsilon_k(h_2)) \\ &\quad \left\{ \frac{(e^{-\beta_H \epsilon_k(h_1)} - e^{\beta_H \epsilon_k(h_1)})}{Z(h_1)} - \frac{(e^{-\beta_C \epsilon_k(h_2)} - e^{\beta_C \epsilon_k(h_2)})}{Z(h_2)} \right\} \end{aligned} \quad (\text{A13})$$

resulting to

$$\begin{aligned} \eta_{adia} &= \quad (\text{A14}) \\ &= \frac{\sum_k \epsilon_k(h_2) \left\{ \frac{(e^{-\beta_H \epsilon_k(h_1)} - e^{\beta_H \epsilon_k(h_1)})}{Z(h_1)} - \frac{(e^{-\beta_C \epsilon_k(h_2)} - e^{\beta_C \epsilon_k(h_2)})}{Z(h_2)} \right\}}{\sum_k \epsilon_k(h_1) \left\{ \frac{(e^{-\beta_H \epsilon_k(h_1)} - e^{\beta_H \epsilon_k(h_1)})}{Z(h_1)} - \frac{(e^{-\beta_C \epsilon_k(h_2)} - e^{\beta_C \epsilon_k(h_2)})}{Z(h_2)} \right\}} \end{aligned}$$

Appendix B: BEQE using LTIM WM

With LTIM as the WM of the quantum Otto cycle, the transverse field B_x is changed from h_1 to h_2 value during the unitary strokes. Following the technique presented here, bath engineering can be implemented by evaluating the corresponding Δ^* using the Kibble Zurek mechanism, and then choosing appropriate cut-off for bath spectral functions such that energy gaps which are less than Δ^* do not participate in the dynamics. LTIM falls under the same universality class as that of TIM.

Let us discuss implementation of single stroke bath engineering in LTIM. When doing bath engineering, some levels will not be allowed to thermalize depending upon the energy gap. There are 2^L energy levels for a system size L and thus $2^L - 1$ energy gaps. Those energy levels having gaps less than the threshold value of $\Delta^* = \left(\frac{\nu z(h_1 - h_2)}{\tau}\right)^{\frac{\nu z}{1 + \nu z}}$ will not thermalize. On the other hand, those with energy gap greater than $\left(\frac{\nu z(h_1 - h_2)}{\tau}\right)^{\frac{\nu z}{1 + \nu z}}$ will thermalize according to the equation

$$p_i = p_{i-1} e^{-(E_i - E_{i-1})/T} \quad (\text{B1})$$

where p_i and p_{i-1} are the populations in the i^{th} and $(i-1)^{\text{th}}$ energy levels.

- In the $\mathbf{C} \rightarrow \mathbf{D}$ non-unitary stroke, the Hamiltonian is with transverse field h_2 . The energy gaps are compared with the Δ^* value. Those energy levels having gaps greater than Δ^* are allowed to interact with the decaying bath in the $\mathbf{C} \rightarrow \mathbf{D}$ stroke and thus thermalize according to

$$\frac{p_{i+1}^D}{p_i^D} = e^{-(E_{i+1} - E_i)/T_c} \quad (\text{B2})$$

where $E_{i+1} - E_i > \Delta^*$.

In order to apply bath engineering in case of gaps that are less than Δ^* i.e, when $E_{i+1} - E_i < \Delta^*$ we have two possibilities;

- If $E_i - E_{i-1} > \Delta^*$, the populations are determined by the condition

$$p_i^D + p_{i-1}^D = p_i^C + p_{i-1}^C. \quad (\text{B3})$$

- If $E_i - E_{i-1} < \Delta^*$, the i^{th} level doesnot interact with any other level leading to $p_i^D = p_i^C$.

Solving these system of equations along with the condition that $\sum_i p_i^D = 1$, we get the population of all the other energy levels at \mathbf{D} . Thus we have ρ^D which is the state reached after doing bath engineering.

- From \mathbf{D} to \mathbf{A} , h_2 is changed back to h_1 from ρ^D using the evolution equation

$$\frac{d\rho}{dt} = -i[H, \rho] \quad (\text{B4})$$

which gives the new density matrix at \mathbf{A} , ρ^A .

- At \mathbf{A} , the system with Hamiltonian $H(h_1)$ is connected to the energizing bath. All energy levels interact with each other resulting in the steady state at \mathbf{B} .
- $\mathbf{B} \rightarrow \mathbf{C}$ stroke, h_1 changed to h_2 by evolving the system from ρ^B to obtain ρ^C .

Now, for the bath engineered engine,

$$Q'_{in} = E_B - E'_A \quad (\text{B5})$$

$$Q'_{out} = E'_D - E_C \quad (\text{B6})$$

$$\mathcal{W}' = -(Q'_{in} + Q'_{out}) \quad (\text{B7})$$

$$\eta' = \mathcal{W}' / Q'_{in} \quad (\text{B8})$$

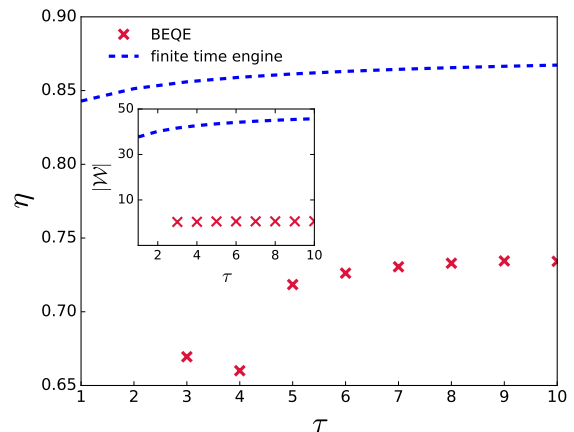


FIG. 7. η is plotted as a function of τ for the BEQE using LTIM as WM compared with finite time engine. Inset: $|\mathcal{W}|$ as a function of τ . The parameters used are $L = 6, h_1 = 10, h_2 = 0.75, T_H = 500, T_C = 0.1, \tau_1 = \tau_2 = \tau$.

Numerical analysis suggest bath engineering fails to improve the performance of the engine in this case (see Fig. 7). We have also checked the implementation of bath engineering in both energizing and decaying strokes, which too fails to improve the performance of the engine.

[1] R. Alicki and R. Kosloff, “Introduction to quantum thermodynamics: History and prospects,” in *Thermodynam-*

- New Directions*, edited by F. Binder, L. A. Correa, C. Gogolin, J. Anders, and G. Adesso (Springer International Publishing, Cham, 2018) pp. 1–33.
- [2] S. Vinjanampathy and J. Anders, *Contemporary Physics* **57**, 545 (2016), <https://doi.org/10.1080/00107514.2016.1201896>.
 - [3] J. Gemmer, M. Michel, and G. Mahler, *Quantum thermodynamics: Emergence of thermodynamic behavior within composite quantum systems*, Vol. 784 (Springer, 2009).
 - [4] R. Kosloff, *Entropy* **15**, 2100 (2013).
 - [5] F. Binder, L. A. Correa, C. Gogolin, J. Anders, and G. Adesso, *Fundamental Theories of Physics* **195**, 1 (2018).
 - [6] S. Bhattacharjee and A. Dutta, *The European Physical Journal B* **94**, 239 (2021).
 - [7] N. M. Myers, O. Abah, and S. Deffner, *AVS Quantum Science* **4**, 027101 (2022), <https://doi.org/10.1116/5.0083192>.
 - [8] P. A. Erdman and F. Noé, *npj Quantum Information* **8**, 1 (2022).
 - [9] I. Khait, J. Carrasquilla, and D. Segal, *Phys. Rev. Research* **4**, L012029 (2022).
 - [10] H. T. Quan, Y.-x. Liu, C. P. Sun, and F. Nori, *Phys. Rev. E* **76**, 031105 (2007).
 - [11] V. Mukherjee and U. Divakaran, *Journal of Physics: Condensed Matter* **33**, 454001 (2021).
 - [12] D. Gelbwaser-Klimovsky, W. Niedenzu, and G. Kurizki (Academic Press, 2015) pp. 329–407.
 - [13] V. Mukherjee, A. Zwick, A. Ghosh, X. Chen, and G. Kurizki, *Commun Phys* **2**, 162 (2019).
 - [14] A. del Campo, J. Goold, and M. Paternostro, *Sci. Rep.* **4**, 6208 (2014).
 - [15] A. Hartmann, V. Mukherjee, W. Niedenzu, and W. Lechner, *Phys. Rev. Research* **2**, 023145 (2020).
 - [16] J. Deng, Q.-h. Wang, Z. Liu, P. Hänggi, and J. Gong, *Phys. Rev. E* **88**, 062122 (2013).
 - [17] M. Beau, J. Jaramillo, and A. del Campo, *Entropy* **18**, 168 (2016).
 - [18] A. del Campo, A. Chenu, S. Deng, and H. Wu, “Friction-free quantum machines,” in *Thermodynamics in the Quantum Regime: Fundamental Aspects and New Directions*, edited by F. Binder, L. A. Correa, C. Gogolin, J. Anders, and G. Adesso (Springer International Publishing, Cham, 2018) pp. 127–148.
 - [19] D. Sels and A. Polkovnikov, *Proceedings of the National Academy of Sciences* **114**, E3909 (2017), <https://www.pnas.org/doi/pdf/10.1073/pnas.1619826114>.
 - [20] A. del Campo, M. M. Rams, and W. H. Zurek, *Phys. Rev. Lett.* **109**, 115703 (2012).
 - [21] M. Kolodrubetz, D. Sels, P. Mehta, and A. Polkovnikov, *Physics Reports* **697**, 1 (2017), geometry and non-adiabatic response in quantum and classical systems.
 - [22] S. Sachdev, *Quantum Phase Transitions*, 2nd ed. (Cambridge University Press, 2011).
 - [23] M. Campisi and R. Fazio, *Nature communications* **7**, 1 (2016).
 - [24] Y.-Y. Chen, G. Watanabe, Y.-C. Yu, X.-W. Guan, and A. del Campo, *npj Quantum Information* **5**, 88 (2019).
 - [25] Y.-H. Ma, S.-H. Su, and C.-P. Sun, *Phys. Rev. E* **96**, 022143 (2017).
 - [26] G. Piccitto, M. Campisi, and D. Rossini, arXiv preprint arXiv:2205.09528 (2022).
 - [27] B. S. Revathy, V. Mukherjee, U. Divakaran, and A. del Campo, *Phys. Rev. Research* **2**, 043247 (2020).
 - [28] A. Dutta, G. Aeppli, B. K. Chakrabarti, U. Divakaran, T. F. Rosenbaum, and D. Sen, *Quantum phase transitions in transverse field spin models: from statistical physics to quantum information* (Cambridge University Press, Cambridge, 2015).
 - [29] A. Polkovnikov, K. Sengupta, A. Silva, and M. Vengalattore, *Rev. Mod. Phys.* **83**, 863 (2011).
 - [30] J. Dziarmaga, *Advances in Physics* **59**, 1063 (2010), <https://doi.org/10.1080/00018732.2010.514702>.
 - [31] M. Keck, S. Montangero, G. E. Santoro, R. Fazio, and D. Rossini, *New Journal of Physics* **19**, 113029 (2017).
 - [32] H. P. Breuer and F. Petruccione, *The Theory of Open Quantum Systems* (Oxford University Press, 2002).
 - [33] S. Deng, G. Ortiz, and L. Viola, *Phys. Rev. B* **83**, 094304 (2011).
 - [34] W. H. Zurek, U. Dorner, and P. Zoller, *Phys. Rev. Lett.* **95**, 105701 (2005).
 - [35] A. Polkovnikov, *Phys. Rev. B* **72**, 161201 (2005).
 - [36] B. Damski and W. H. Zurek, *Phys. Rev. A* **73**, 063405 (2006).
 - [37] E. Lieb, T. Schultz, and D. Mattis, *Annals of Physics* **16**, 407 (1961).
 - [38] P. Pfeuty, *Annals of Physics* **57**, 79 (1970).
 - [39] J. E. Bunder and R. H. McKenzie, *Phys. Rev. B* **60**, 344 (1999).
 - [40] S. Bandyopadhyay, S. Laha, U. Bhattacharya, and A. Dutta, *Scientific Reports* **8**, 11921 (2018).
 - [41] A. del Campo, M. M. Rams, and W. H. Zurek, *Phys. Rev. Lett.* **109**, 115703 (2012).
 - [42] J. Roßnagel, S. T. Dawkins, K. N. Tolazzi, O. Abah, E. Lutz, F. Schmidt-Kaler, and K. Singer, *Science* **352**, 325 (2016).
 - [43] S. Ulm, J. Roßnagel, G. Jacob, C. Degünther, S. T. Dawkins, U. G. Poschinger, R. Nigmatullin, A. Retzker, M. B. Plenio, F. Schmidt-Kaler, and K. Singer, *Nat. Comm.* **4**, 2290 (2013).
 - [44] K. Pyka, J. Keller, H. L. Partner, R. Nigmatullin, T. Burgermeister, D. M. Meier, K. Kuhlmann, A. Retzker, M. B. Plenio, W. H. Zurek, A. del Campo, and T. E. Mehlstäubler, *Nat. Comm.* **4**, 2291 (2013).
 - [45] G. Maslennikov, S. Ding, R. Hablützel, J. Gan, A. Roulet, S. Nimmrichter, J. Dai, V. Scarani, and D. Matsukevich, *Nature Communications* **10**, 202 (2019).
 - [46] D. von Lindenfels, O. Gräß, C. T. Schmiegelow, V. Kaushal, J. Schulz, M. T. Mitchison, J. Goold, F. Schmidt-Kaler, and U. G. Poschinger, *Phys. Rev. Lett.* **123**, 080602 (2019).
 - [47] M. Schreiber, S. S. Hodgman, P. Bordia, H. P. Lüschen, M. H. Fischer, R. Vosk, E. Altman, U. Schneider, and I. Bloch, *Science* **349**, 842 (2015).
 - [48] J. Klatzow, J. N. Becker, P. M. Ledingham, C. Weinzetl, K. T. Kaczmarek, D. J. Saunders, J. Nunn, I. A. Walmsley, R. Uzdin, and E. Poem, *Phys. Rev. Lett.* **122**, 110601 (2019).
 - [49] J. P. S. Peterson, T. B. Batalhão, M. Herrera, A. M. Souza, R. S. Sarthour, I. S. Oliveira, and R. M. Serra, *Phys. Rev. Lett.* **123**, 240601 (2019).
 - [50] J.-M. Cui, F. J. Gómez-Ruiz, Y.-F. Huang, C.-F. Li, G.-C. Guo, and A. del Campo, *Communications Physics* **3**, 44 (2020).
 - [51] S. Sharma, S. Suzuki, and A. Dutta, *Phys. Rev. B* **92**, 104306 (2015).
 - [52] O. de Alcantara Bonfim, B. Boechat, and J. Florencio,

